

Supplementary Information:

Understanding the solvent-assisted crystallization mechanism inherent in efficient organic-inorganic halide perovskite solar cells

Dinghan Shen,^a Xiao Yu,^a Xin Cai,^a Ming Peng,^a Yingzhuang Ma,^b Xin Su,^a Lixin Xiao*^b and
Dechun Zou*^{a, c}

^a Beijing National Laboratory for Molecular Sciences, Key Laboratory of Polymer Chemistry and Physics of Ministry of Education, College of Chemistry and Molecular Engineering, Peking University, Beijing, 100871, China. E-mail: dczou@pku.edu.cn

^b State Key Laboratory for Mesoscopic Physics and Department of Physics, Peking University, Beijing 100871, PR China. E-mail: xiao66@pku.edu.cn

^c Beijing Institute of Nanoenergy and Nanosystems, Chinese Academy of Science.

1. Experimental details:

Materials and preparation of precursor solutions: Methylammonium iodide ($\text{CH}_3\text{NH}_3\text{I}$) was synthesized by reacting the mixture of hydroiodic acid and methylamine with the method described by Michael M. Lee, *et. al.* DMF-based or DMAc-based precursor solution was prepared by dissolving $\text{CH}_3\text{NH}_3\text{I}$ and PbI_2 mixture (molar ratio of 3:1) in either DMF or DMAc with the same concentration of 40 wt%.

Fabrication of PHJ perovskite devices: Perovskite-based PHJ solar cells are fabricated as follows: FTO glass substrates were sequentially cleaned ultrasonically with deionized water, acetone and ethanol, followed by oxygen plasma treatment for 15 min. A TiO_2 blocking layer was then deposited onto cleaned FTO substrate by spin coating a mildly acidic solution of titanium isopropoxide in ethanol adopted by A. Abrusci. *et. al.* After drying at 125 °C for 15 min, a second blocking layer was further spin coated to prevent shunting, followed by sintering at 500 °C for 30 min. Perovskite thin films were then spin coated from 40 wt% DMF-based precursor solution at 2000 rpm for 30 s and annealed at 100 °C for 60 min. Afterward, the hole-transporting layer was deposited by spin coating 2,2',7,7'-Tetrakis[N,N-di(4-methoxyphenyl)amino]-9,9'-spirobifluorene (Spiro-OMeTAD) at 2000 rpm for 60 s, where the solution was prepared by dissolving 72.3 mg of Spiro-OMeTAD in 1mL of chlorobenzene with additives described by Julian Burschka *et. al.* Finally, gold electrode with thickness of 75 nm was formed via magnetron sputtering to finish the PHJ devices. To facilitate comparison, DMAc-based devices were fabricated with the identical procedure except for the utilization of DMAc as the precursor solvent. The DMF vapor post-treatment was achieved via dropping 5mL of DMF around the formed perovskite thin film under room temperature and promptly covering it with a glass petri dish for several minutes.

Characterization of the precursor film: DMF- and DMAc-induced precursor films for infrared spectroscopy and X-ray diffraction characterizations were prepared by spin coating corresponding precursor solutions on cleaned FTO substrates. Due to the unstable nature of precursor films in ambient atmosphere, apart from the measurement duration of several minutes, we carefully isolated these samples from oxygen and moisture exposure by putting them in preservative plastic bags within a sealed box, and then taking them out from the N_2 -filled glovebox. The composition of chemical bondings was measured by infrared spectroscopy with Bruker, Tensor 27. The crystalline structures of both precursor films and perovskite films were identified by XRD (Bruker, D2 PHASER).

Solar cell characterization: The photovoltaic performances of PHJ devices were measured in ambient on a Keithley Model 2000 under simulated AM 1.5 sunlight generated by a YSS-5A (Yamashita DESO, Japan), whose light intensity was calibrated with a standard silicon solar cell. The active area of solar cell was defined as 3.14 mm^2 . Film morphology of both the blocking layer and the perovskite layer were observed using field emission SEM (S-4800 Hitachi, Japan). The surface undulation of perovskite films was identified by AFM with Nano Scope III.

2. SEM images of single/double blocking layer substrate

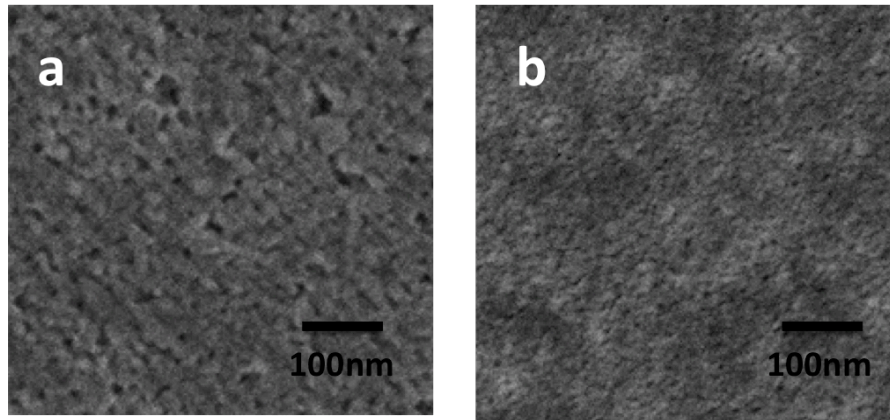


Figure S1. Surface SEM images of (a) single blocking layer, showing obvious pores; (b) double blocking layer, illustrating negligible surface defects.

3. The evolution of DMF molecules' content inside the precursor film

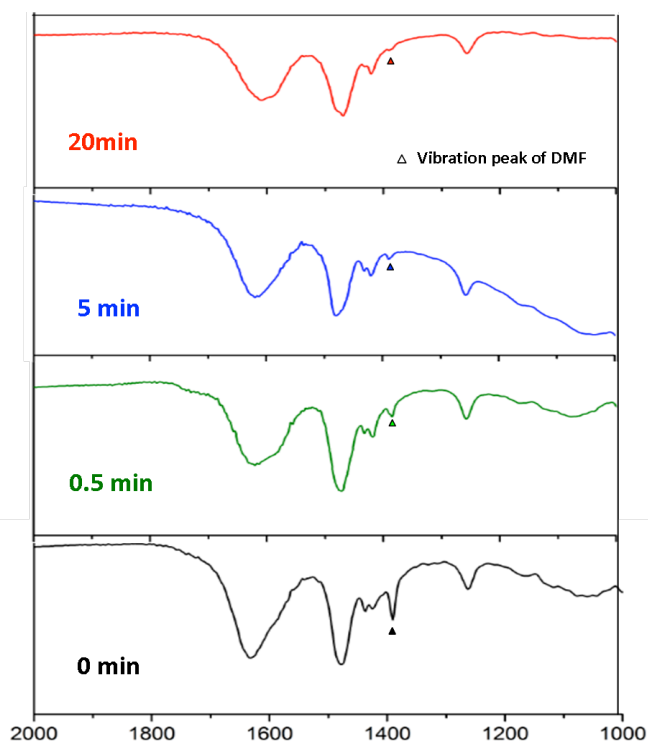


Figure S2. FTIR spectra (from 2000cm^{-1} to 1000cm^{-1}) of DMF-induced precursor films with different annealing times shown on corresponding images. Intensity evolution of the symmetrical C-H bending peak from DMF molecules is specifically marked.

4. Infrared transmittance spectra of relevant chemical compositions

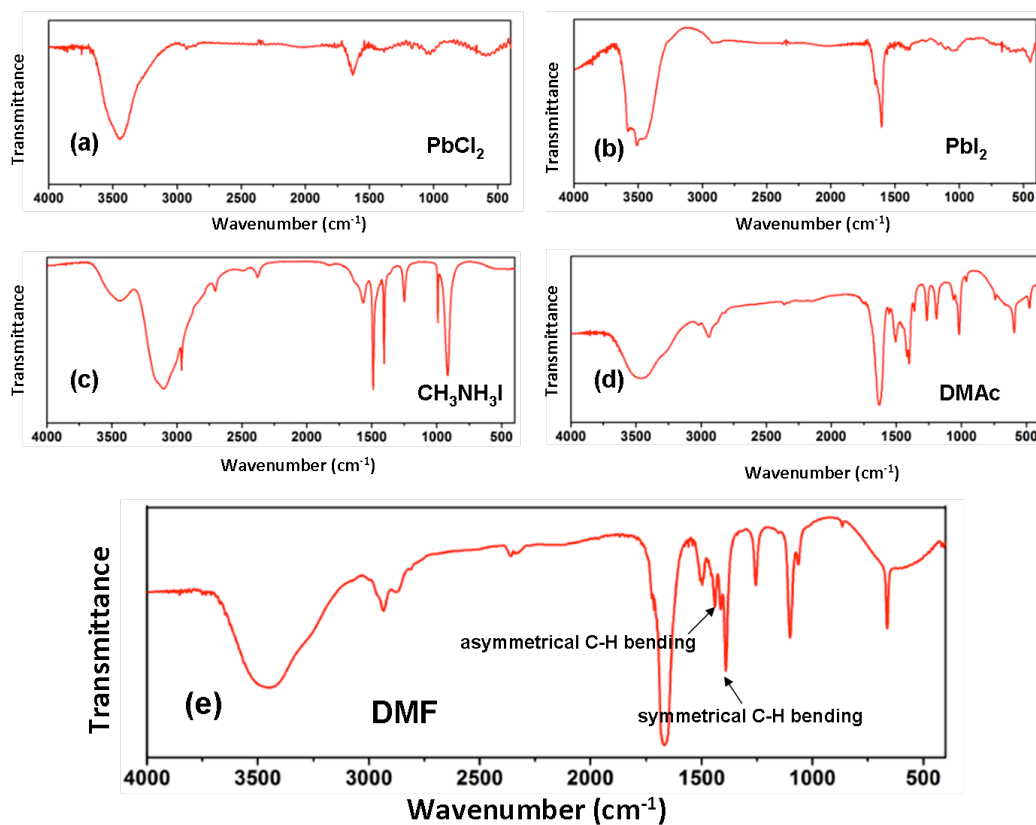


Figure S3. FTIR spectra of (a) PbCl₂, (b) PbI₂, (c) CH₃NH₃I powders; (d) DMAc, (e) DMF solvents.

5. XRD characterization of relevant chemical compositions

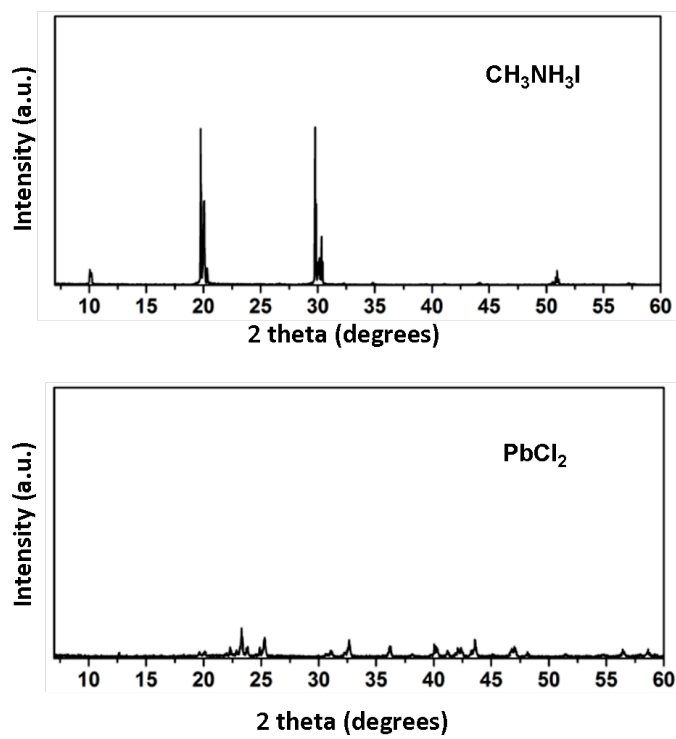


Figure S4. XRD spectra of PbCl_2 , $\text{CH}_3\text{NH}_3\text{I}$ isolated powders.

6. Film morphology of perovskite thin films deposited on different substrates

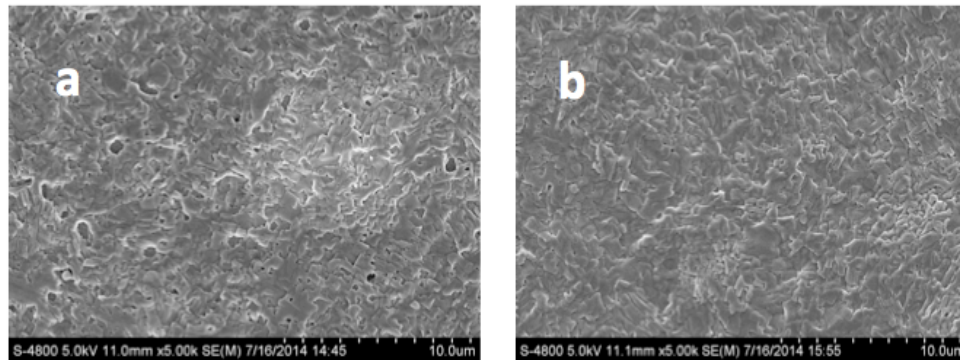


Figure S5. Surface SEM images of perovskite thin films formed on the substrate of (a) single coating of TiO_2 compact layer; (b) double coating of TiO_2 compact layer. The number of active layer pinholes is efficiently cut down due to smoother blocking layer surface.

7. The color evolution of DMF/DMAc-induced precursor film upon annealing

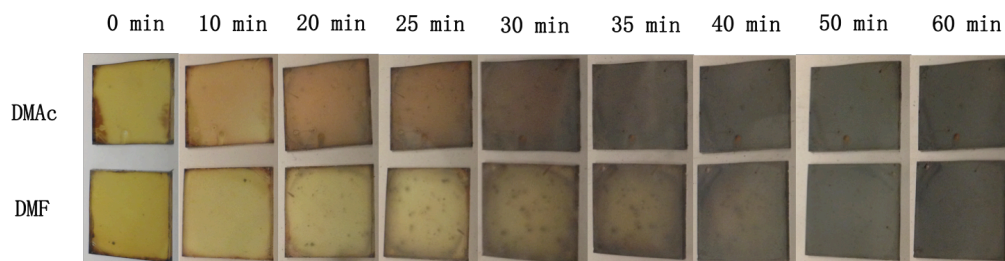


Figure S6. Photographs of DMAc-induced precursor film and DMF-induced precursor film upon annealing at 100 °C for different time. The color transformation of DMF-induced precursor film from yellow to black appears to be much slower.